Experimental and Theoretical Investigation of Solubility and Diffusion of Ethylene in Semicrystalline PE at Elevated Pressures and Temperatures

C. Kiparissides, V. Dimos, T. Boultouka, A. Anastasiadis, A. Chasiotis

Department of Chemical Engineering and Chemical Process Engineering Research Institute, Aristotle University of Thessaloniki, P.O. Box 472, 54006 Thessaloniki, Greece

Received 30 November 2001; accepted 18 March 2002

ABSTRACT: The solubility and diffusivity of ethylene in semicrystalline polyethylene were experimentally measured using a magnetic suspension microbalance. The sorption measurements were carried out at temperatures up to 80°C and pressures up to 66 atm. The experimentally measured solubilities were found to decrease with increasing temperature and increased with ethylene pressure in good agreement with the predictions of the Sanchez–Lacombe lattice-fluid model. The diffusivity of ethylene in semicrystalline polyethylene films was estimated from the reduced sorption curves using the half-time method. The experimentally determined diffusivities were compared with theoretical values predicted by a new molecular hybrid model, which combines the characteristic features of the Pace–Datyner diffusion model with those of the Kulkarni–Stern free-volume model. The ethylene diffusion coefficient was found to increase with temperature and/or the ethylene-sorbed concentration. © 2002 Wiley Periodicals, Inc. J Appl Polym Sci 87: 953–966, 2003

Key words: ethylene solubility; ethylene diffusivity; polyethylene (PE); modeling; thermodynamics

INTRODUCTION

In heterogeneous Ziegler–Natta catalytic olefin polymerization, the polymerization rate and, thus, the growth of a polymer particle will depend on the catalyst's activity and the concentration of the sorbed monomer at the catalyst active sites. One of the most important parameters in predicting the growth of a catalyst particle is the monomer diffusion coefficient in the polymer phase. In general, the monomer diffusivity will be a complex function of particle morphology (e.g., particle porosity), microstructure of polymer chains (e.g., molecular weight distribution, copolymer composition, degree of crystallinity), and temperature. Thus, the experimental measurement of monomer solubility and diffusion coefficient is of profound importance for the catalytic polyolefin industry. The present investigation was undertaken in response to an urgent need for accurate data on solubility and diffusivity of small molecules (e.g., C_2H_4, C_3H_8, H_2, etc.) in polyolefins, at elevated pressures and temperatures.

A great number of experimental and theoretical studies, dealing with the solubility of gases and vapors in polyethylene, have been reported in the open literature. Michaels and Parker[1] and Michaels and Bixler[2] studied the effect of polymer morphology on the solubility of small gaseous molecules such as nitrogen, oxygen, and carbon dioxide in semicrystalline polyethylene (PE). They reported that, at low pressures, the solubility of the particular gases followed the Henry's law. Rogers et al.[3] were among the first investigators who measured the equilibrium sorption of heavy organic vapors (e.g., *n*-hexane, *n*-heptane, benzene) in semicrystalline PE films by means of a quartz helix microbalance. They proposed a simple empirical exponential correlation to describe the dependence of the vapor solubility coefficient on the concentration of the penetrant molecules. Li and Long[4] determined experimentally the solubilities of nitrogen, methane, and ethylene in semicrystalline PE at pressures up to 90 atm and showed that the solubility of ethylene increased exponentially with increasing pressure. Beret and Hager[5] measured the solubility of ethylene in semicrystalline PE films at atmospheric pressure. Kulkarni and Stern[6] measured the equilibrium mass uptake of CO_2, CH_4, C_2H_4, and C_3H_8 by semicrystalline PE rods at gas pressures up to 40 atm and found that the solubility coefficient of all penetrants remained constant and within the Henry's law limits, regardless of gas pressure. Castro et al.[7] measured the solubility of *n*-butane, *n*-pentane, *n*-hexane, and *n*-heptane in PE membranes at very low pressures (<1 atm) and used the Flory–Huggins theory to analyze their experimental results. Hutchinson[8] showed that the solubility coefficient of various gases and vapors (e.g., ethane, methane, ethylene, propylene) in semicrystalline PE followed the Henry's

Correspondence to: C. Kiparissides (cypress@alexandros.cperi.certh.gr).

Journal of Applied Polymer Science, Vol. 87, 953–966 (2003)
© 2002 Wiley Periodicals, Inc.

law. Yoon et al.[9] determined experimentally the solubility of ethylene and *a*-olefin in ethylene/*a*-olefin random copolymers by means of a quartz spring at pressures up to 1.3 atm. Nath and de Pablo[10] employed Monte Carlo simulations to study the solubility of ethylene in PE. The theoretically calculated gas solubilities deviated from the experimental results of Li and Long[4] by more than 100%. Finally, Sato et al.[11] measured the solubility of CO_2 and N_2 in molten PE at pressures up to 167.8 atm by using a pressure decay method. They employed the Sanchez–Lacombe equation of state to correct their experimental measurements for polymer swelling.

The diffusion of gases and vapors in polymers has been the subject of a great number of studies. In 1957, Barrer[12] reviewed the diffusion properties of gases in polymers. Fujita[13] employed the Cohen–Turnbull free-volume theory[14] to correlate experimental diffusivity data of benzene in polyethyl acrylate. Michaels and Bixler[15] measured the diffusivities of several gases (e.g., CO_2, N_2, O_2, and CH_4) in semicrystalline PE as a function of temperature and the degree of crystallinity. Rogers et al.[3] investigated experimentally the diffusion of organic vapors (e.g., *n*-hexane, *n*-heptane, benzene) in semicrystalline PE and attributed the increase in the diffusion coefficient with concentration of polymer swelling caused by the diffusing species. Robeson and Smith[16] showed that the experimentally measured diffusivities of ethane–butane mixtures followed an exponential dependence with respect to the butane concentration. Pace and Datyner[17–19] proposed a molecular model to describe the diffusion of simple molecules in polymers based on the physicochemical properties of the polymer–gas system. Vrentas and Duda,[20] on the other hand, developed a general free-volume theory to account for the dependence of the diffusion coefficient of small molecules in amorphous polymers on temperature and the penetrant concentration. Kreituss and Frisch[21] measured the diffusivities of CCl_4, benzene, and *n*-hexane in semicrystalline ethylene–propylene copolymers by means of a quartz helix spring balance. They employed a modified Fujita-like free-volume model to determine the effects of concentration and crystallinity on the diffusion coefficient. Kulkarni and Stern[6] employed the free-volume model of Kreituss and Frisch[21] to analyze their own experimental data on the diffusion of CO_2, CH_4, C_2H_4, and C_3H_8 in semicrystalline PE. Doong and Ho[22] studied the diffusion of a series of aromatic hydrocarbons (e.g., benzene, toluene) in semicrystalline PE by means of a gravimetric sorption technique. They developed a diffusion model that combined the key features of the Pace–Datyner molecular theory with the Vrentas–Duda's free-volume approach. In a recent review by Schlotter and Furlan,[23] the diffusion of small molecules in polyolefins was reported. Yoon et al.[9] determined experimentally the diffusion coefficients of ethylene and *a*-olefin in random copolymers by means of a quartz spring. Finally, Sato et al.[11] employed an exponential-type correlation to account for the dependence of the gas diffusivity in random copolymers on the penetrant concentration.

The scope of the present study was to determine both experimentally and theoretically the solubility and the diffusion coefficients of ethylene in semicrystalline PE at elevated pressures and temperatures. A Rubotherm magnetic suspension microbalance was used to measure the equilibrium ethylene mass uptake by semicrystalline PE films. The Sanchez–Lacombe equation of state was employed to calculate the equilibrium ethylene solubility in PE with respect to temperature and ethylene pressure. Finally, a molecular hybrid diffusion model was developed to predict the ethylene diffusivity in terms of temperature, the concentration of the penetrant molecules, and the degree of polymer crystallinity.

CALCULATION OF THE GAS/VAPOR SOLUBILITY COEFFICIENT

Semicrystalline polymers are generally considered to consist of two phases, namely, an amorphous phase that allows the passage of penetrant molecules, and a crystalline one that acts as barrier to the diffusion of penetrant molecules. Since semicrystalline polymers sorption occurs only in the amorphous polymer phase,[1,2] the solubility coefficient, S, defined as the ratio of the mass of sorbed gas or vapor over the total polymer mass, will be given by

$$S = \omega_\alpha S^* \tag{1}$$

where S^* is the equilibrium solubility coefficient of the penetrant molecules in the amorphous polymer phase (e.g., mass fraction of the sorbed monomer over the amorphous polymer mass) and ω_α is the amorphous mass fraction in the semicrystalline polymer. In eq. (1), it is assumed that the degree of polymer crystallinity has no effect on the gas/vapor solubility in the amorphous polymer phase.

Hutchinson and Ray,[24] by analyzing available experimental solubility data on the sorption of different gases and vapors in semicrystalline PE, concluded that a Henry's law correlation could be employed to calculate the gas/vapor solubility in amorphous PE in terms of the partial pressure of the penetrant

$$[M]^* = k^* P \tag{2}$$

where $[M]^*$ is the concentration of the sorbed molecules in the amorphous polymer, P is the partial pressure of the gas/vapor, and k^* is the Henry's law constant.

Stern et al.[25] showed that the Henry's law constant, at zero penetrant concentration, can be related to the critical temperature of the penetrant gas or vapor, T_c.

Specifically, Hutchinson[24] found that, for gases and vapors in semicrystalline PE, the Henry's law constant could be expressed as:

$$\log(k^*) = -2.38 + 1.08(T_c/T)^2 \quad (3)$$

At elevated pressures and/or for heavier hydrocarbons, the solubility coefficient can deviate from Henry's law . Rogers et al.[3] employed an exponential-type relationship with respect to the concentration of the penetrant molecules, C, to calculate the equilibrium solubility coefficient of heavier than ethylene organic vapors (e.g., pentane, benzene, etc.) in PE, and

$$S^*(C) = k^* \exp(bC) \quad (4)$$

where b is a positive constant. In general, an equation of the stated model can be employed to predict the equilibrium concentration of the sorbed penetrant molecules in the amorphous polymer phase. Chen[26] used the Heuer–Schotte equation of state to calculate the sorption of hydrocarbon vapors in amorphous PE. Orbey et al.[27] employed the Sanchez–Lacombe equation of state to calculate the phase equilibrium of a binary ethylene–PE mixture in a low-density PE process. They showed that the Sanchez–Lacombe equation of state can predict the ethylene–PE phase equilibrium as long as the binary interaction parameters are correctly selected. Briskoe et al.[28] used the Sanchez–Lacombe equation of state to predict the sorption of CO_2 in semicrystalline PVDF at pressures up to 296 atm.

In the present study, the Sanchez–Lacombe (S–L) lattice-fluid model[29–31] was employed to calculate the equilibrium concentration of sorbed ethylene in amorphous PE. Following the original developments of Sanchez and Lacombe, the general equation of state is written,

$$\tilde{\rho}^2 + \tilde{P} + \tilde{T}\left[\ln(1-\tilde{\rho}) + \left(1 - \frac{1}{r}\right)\tilde{\rho}\right] = 0 \quad (5)$$

where $\tilde{T}$, $\tilde{P}$, and $\tilde{\rho}$ are the reduced temperature, pressure, and density of a pure substance, respectively, defined as

$$\tilde{T} = T/T^*; \quad \tilde{P} = P/P^*; \quad \tilde{\rho} = \rho/\rho^* = 1/\tilde{v} = V^*/V \quad (6)$$

where T, P, ρ, and V denote the absolute temperature, pressure, density, and molar volume of a pure substance, respectively. The number of sites (mers) a molecule occupies in the lattice, r, can be related to the molecular weight of the pure component, M, according to the equation:

$$r = P^*M/(RT^*\rho^*) \quad (7)$$

Notice that for a high molecular weight polymer the value of r is considered to be infinite. The characteristic parameters, P^*, T^*, ρ^*, V^*, are defined as[32]

$$T^* = \varepsilon^*/R; \quad P^* = \varepsilon^*/v^*; \quad V^* = N(rv^*); \quad \rho^* = M/(rv^*) \quad (8)$$

where ε^* is the mer–mer interaction energy, v^* is the closed-packed molar volume of a mer, N is the number of molecules, and R is the universal gas constant. For a pure substance, the values of the parameters P^*, T^*, and ρ^* can be determined by fitting the Sanchez–Lacombe equation of state to known experimental PVT data.

For a polymer–vapor mixture, it is necessary to use a combined mixing rule for the calculation of $\varepsilon^*_{\text{mix}}$, v^*_{mix}, and r_{mix} based on the corresponding values of the pure-component parameters. Thus, by using the van der Waals-1 mixing rule, the characteristic close-packed molar volume of a mer in the mixture, v^*_{mix}, can be defined as

$$v^*_{\text{mix}} = \sum_{i=1}\sum_{j=1} \varphi_i\varphi_j v^*_{ij} \quad (9)$$

where

$$v^*_{ij} = \frac{v^*_{ii} + v^*_{jj}}{2}(1 - n_{ij}) \quad (10)$$

The parameter n_{ij} accounts for possible deviation of v^*_{ij} from the arithmetic mean of the corresponding values v^*_{ii} and v^*_{jj} of the pure components. Accordingly, the average values of $\varepsilon^*_{\text{mix}}$ and r_{mix} of the mixture can be calculated by the equations

$$\varepsilon^*_{\text{mix}} = \frac{1}{v^*_{\text{mix}}}\sum_{i=1}\sum_{j=1} \varphi_i\varphi_j[(\varepsilon^*_{ii}\varepsilon^*_{jj})^{0.5}(1 - k_{ij})]v^*_{ij} \quad (11)$$

$$r^{-1}_{\text{mix}} = \sum_{j=1} (\varphi_j/r_j) \quad (12)$$

where k_{ij} is a binary interaction parameter for the i and j components in the mixture. The volume fraction of the i component in the mixture, φ_i, can be expressed in terms of the mass fraction m_i and the characteristic values v^*_i and ρ^*_i of the pure components:

$$\varphi_i = \frac{m_i}{\rho^*_i v^*_i}\left[\sum_{j=1}\left(\frac{m_j}{\rho^*_j v^*_j}\right)\right]^{-1} \quad (13)$$

Following the developments of McHugh and Krukonis,[32] the chemical potential of the i component in a multicomponent system can be expressed as

$$\mu_i = RT\left[\ln \varphi_i + \left(1 - \frac{r_i}{r}\right)\right] + r_i\left\{\begin{array}{l} -\tilde{\rho}\left[\dfrac{2}{\nu^*}\left(\displaystyle\sum_{j=1}^{N_c} \varphi_j \nu_{ij}^* \varepsilon_{ij}^* - \varepsilon^* \sum_{j=1}^{N_c} \varphi_j \nu_{ij}^*\right) + \varepsilon^*\right] \\ +RT\tilde{\nu}\left[(1-\tilde{\rho})\ln(1-\tilde{\rho}) + \dfrac{\tilde{\rho}}{r_i}\ln\tilde{\rho}\right] + P\tilde{\nu}\left(2\displaystyle\sum_{j=1}^{N_c} \varphi_j \nu_{ij}^* - \nu^*\right) \end{array}\right\} \quad (14)$$

where N_c denotes the number of components in the mixture. For a binary polymer–gas (or vapor) system at equilibrium, the chemical potentials of each component in the two phases will be equal:

$$\mu_i^{\text{polymer}} = \mu_i^{\text{gas}} \quad (15)$$

Thus, at a given ethylene pressure and temperature, the volume fraction of ethylene in the polymer phase, φ_1, can be calculated from eq. (15) by using a nonlinear equation solver software package (e.g., GREG). Accordingly, the mass fraction of ethylene in the amorphous polymer phase can be calculated from eq. (13). Finally, the equilibrium ethylene solubility coefficient in the amorphous PE is computed by:

$$S^* = m_1/m_2 \quad (16)$$

An explanation of all symbols appearing in the above equations can be found in the nomenclature of this article.

CALCULATION OF THE EFFECTIVE DIFFUSION COEFFICIENT

In interpreting diffusion data of small molecules in semicrystalline polymers, one should carefully account for the local interactions between the polymer chains and the gaseous penetrant molecules, the extent of polymer crystallinity, as well as for polymer swelling induced by the sorbed gas or vapor. In general, the effective diffusion coefficient of the penetrant molecules in semicrystalline polymers will depend on temperature, the concentration of sorbed molecules, and the degree of crystallinity. According to Doong and Ho,[22] the diffusion of complex molecules in polymers can be expressed as a product of the thermodynamic diffusion coefficient at zero penetrant concentration, $D_d(d, T, \varphi_c)$, and a factor that accounts for the concentration and size of the penetrant molecules. Similarly, in the proposed hybrid model, the effective diffusion coefficient, D_{eff}, is expressed as the product of three terms

$$D_{\text{eff}}(d, T, \varphi_1, \varphi_c) = D_d(d, T, \varphi_c) * f(\varphi_1, \varphi_c) * g(\varphi_1) \quad (17)$$

where $f(\varphi_1, \varphi_c)$ is a correction function accounting for the plasticizing effect of the sorbed penetrant, and $g(\varphi_1)$ accounts for the net bulk flow of the polymer-penetrant system. The symbols d, φ_1, and φ_c denote the diameter of the spherical penetrant molecules, the volume fraction of sorbed gas/vapor in the amorphous polymer phase, and the volume fraction of the crystalline phase, respectively.

Pace and Datyner[17–19] developed a molecular model, based on the local interactions between the polymer chain segments and the penetrant molecules, to predict the thermodynamic diffusion coefficient of simple molecules in amorphous polymers as a function of temperature. Following DiBenedetto's developments, Pace and Datyner assumed an approximately semicrystalline order in the amorphous polymer regions. The chain bundles were considered to be locally parallel along distances of several nanometers. A coordination number of 4 was assigned for the amorphous regions, in contrast to the coordination number of 6 corresponding to crystalline closest packing. Thus, according to the Pace and Datyner model, a penetrant molecule can move through the amorphous polymer phase in two distinct ways: (i) along the axis of a tube formed by adjacent parallel chains, and (ii) perpendicular to this axis. The latter move can be affected if the polymer chains are sufficiently separated to permit passage of the penetrant molecule. Thus, the minimum separation distance between the polymer chains equals the diameter of the diffusing molecule. Based on the above assumptions, Pace and Datyner[17,33] derived the following equation to express the dependence of the thermodynamic diffusion coefficient of simple molecules on the physical and molecular properties of the polymer-penetrant system,

$$D_d(d, T, \varphi_c) = (9.10 * 10^{-4})\,\frac{\bar{L}^2}{\lambda^2}\left(\frac{E^*}{l^*}\right)^{5/4}\left(\frac{\sqrt{\beta}}{m^*}\right)^{1/2} \times \frac{d'}{\partial\Delta E/\partial d}\exp(-\Delta E/RT) \quad (18)$$

where

$$\Delta E = 5.23\left(\frac{\beta}{d'}\right)^{1/4}\left(\frac{E^* l^*}{\lambda^2}\right)^{3/4}\left\{0.077\left[\left(\frac{l^*}{l}\right)^{11}(\rho - 10d') - l^*\left(\frac{l^*}{l^* + d}\right)^{10}\right] - 0.58\left[\left(\frac{l^*}{l}\right)^{5}(l - 4d') - l^*\left(\frac{l^*}{l^* + d}\right)^{4}\right]\right\}^{3/4} \quad (19)$$

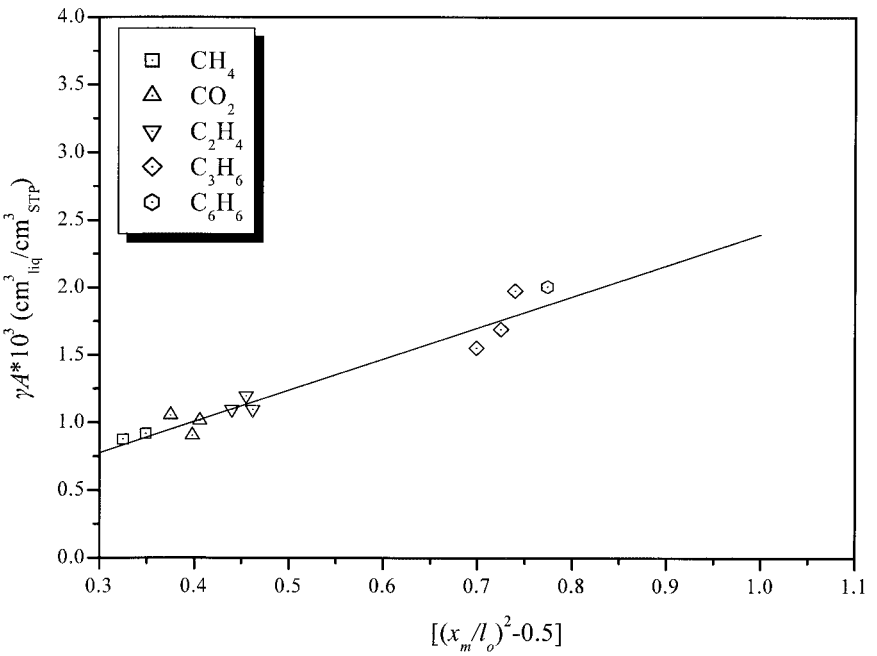

Figure 1 Predicted and experimental values of the concentration coefficient, γ.

where E^* and l^* are the average Lennard–Jones energy and distance parameters of a backbone element, respectively, λ is the mean backbone element separation measured along the chain axis, β is the average effective single chain-bending modulus per unit length, which is a function of the chain geometry. d' $(= d + l^* - l)$ is an equivalent diameter of the penetrant molecule, l is the equilibrium chain separation distance, and m^* is the molecular weight per polymer backbone element. ΔE is the minimum energy required for an effective separation of polymer chains equal to the penetrant diameter.[17] $\bar{L}$ is the distance traveled by the diffusing molecules along the axis of polymer chains until a barrier such as an entanglement, a crosslink, or a crystallite is reached. Although $\bar{L}$ cannot be generally predicted within the limits of this theory, typical values of $\bar{L}$ have been reported[19] for various gases as a function of ΔE and the degree of PE crystallinity.

Based on the free-volume theory,[21] Kulkarni and Stern[6] investigated the dependence of diffusion coefficient on the concentration of the penetrant molecules. Kulkarni and Stern concluded that the effect of the penetrant concentration on the diffusion coefficient could be expressed by the exponential free-volume relationship

$$f(\varphi_1, \varphi_c) = \exp\left[\frac{B_d \gamma \varphi_1}{V_f^*(T) V_f(T, \varphi_1)(1 - \varphi_c)}\right] \qquad (20)$$

where V_f^* is the fractional free volume of the polymer, defined as

$$V_f^*(T) = V_{fg} + \alpha(T - T_g) \qquad (21)$$

where T_g and V_{fg} are the glass transition temperature and the fractional free volume of the polymer at T_g, respectively. The value of V_{fg} is usually taken to be equal to 0.025.[6] α is the thermal expansion coefficient of polymer. For amorphous polyethylene,[21] the value of α will be equal to 7×10^{-4} °C^{-1}. B_d is a parameter related to the relative sizes of the penetrant molecules and polymer segments. Finally, γ is a concentration coefficient, which accounts for the contribution of the penetrant volume fraction, φ_1, to the total free volume of the system:

$$V_f(T, \varphi_1) = V_f^*(T) + \gamma\varphi_1 \qquad (22)$$

According to Kulkarni and Stern,[6] the thermodynamic diffusion coefficient at zero penetrant concentration will be given by the expression:

$$\ln\left(\frac{D_d}{RT}\right) = \ln A_d - \frac{B_d}{V_f^*(1 - \varphi_c)} \qquad (23)$$

The characteristic parameters B_d and A_d, appearing in eq. (23), represent the respective slope and intercept of a straight line when the values of $\ln(D_d/RT)$ are plotted with respect to $1/V_f^*$ at different temperatures. In the present study, eqs. (18) and (21) were employed to calculate the values of D_d and V_f^* at different temperatures. Subsequently, a nonlinear equation solver was used to obtain estimates of B_d and A_d from the calculated values of D_d and V_f^*.

Following the developments of Kulkarni and Stern,[6] a correlation that relates the parameter γ with charac-

teristic molecular parameters of the polymer and penetrant molecules was derived

$$\gamma A * 10^3 = 2.311 * \left[\left(\frac{x_m}{l_0} \right)^2 - 0.5 \right] \qquad (24)$$

where A is the liquid molar volume of the sorbed gas/vapor divided by 22,414 (cm^3_{STP}/mol), x_m is the minimum distance between a penetrant molecule and the nearest chain center of a neighboring polymer chain, and l_0 is the mean separation distance between polymer chains, evaluated from the polymer density.[17] In Figure 1, the validity of eq. (24) is tested for various penetrant gases and vapors in PE. Discrete points represent experimental data reported by Kulkarni and Stern.[6] Apparently, there is good agreement between model predictions and experimental measurements. Thus, using eq. (24) for the estimation of γ, the dependence of diffusion coefficient on the penetrant concentration can be deduced [see eq. (22)].

Finally, the function $g(\varphi_1)$, which accounts for the net bulk flow of the polymer-penetrant systems, is expressed as follows[33]:

$$g(\varphi_1) = (1 - \varphi_1)^3 \qquad (25)$$

EXPERIMENTAL SORPTION MEASUREMENTS

A Rubotherm, three-position magnetic suspension balance was used to measure the mass uptake of ethylene by semicrystalline PE films. The microbalance could measure loads of up to 25 g with an accuracy of 0.01 mg. Its operation capabilities extended over a wide range of pressures (0–300 atm) and temperatures (−20–120°C). A schematic representation of the basic apparatus and its mode of operation are illustrated in Figure 2. As can be seen, the sample basket is not directly connected to the balance plate but is attached to a suspension magnet that is kept in position by the magnetic field of an electromagnet, placed in a separate chamber. The electromagnet is mechanically attached to the balance. Thus, the gravity force that is applied to the sample is transferred via the magnetic suspension coupling of the basket to the balance plate (see Fig. 2). The fact that the sample basket and the balance are placed in two separate chambers makes possible the operation of the microbalance at high pressures and even with corrosive gases or vapors.

In the present study, the measurement of the mass of sorbed ethylene by semicrystalline PE films was carried out under isothermal and isobaric conditions. Polyethylene films of an approximate thickness of 0.4 mm were prepared with the aid of a hot-press apparatus by melting and pressing high-density polyethylene (HDPE) grains at a temperature of about 130°C for 15 min. The mass fraction of crystalline PE phase, ω_c, was measured with a differential scanning calorimeter (DSC).

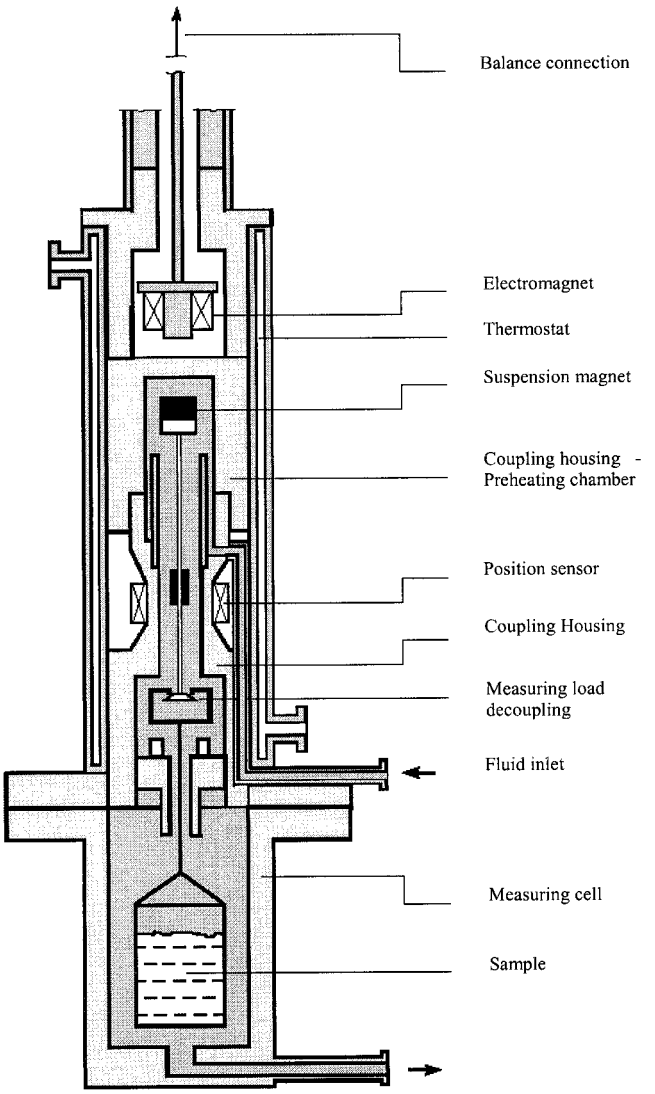

Figure 2 Schematic representation of the Rubotherm magnetic suspension microbalance.

Specifically, by measuring the heat of fusion of a PE film and dividing it by the heat of fusion of 100% crystalline PE (e.g., 64.6 cal/g[9]), the value of ω_c could be determined. From the measured value of ω_c (=0.738) and the densities of crystalline (ρ_c = 0.997 g/ml) and amorphous (ρ_α = 0.854 g/ml) PE, the density of the semicrystalline PE (ρ), could be deduced as

$$\omega_c = \frac{\rho_c}{\rho} \left(\frac{\rho - \rho_\alpha}{\rho_c - \rho_\alpha} \right) \qquad (26)$$

Accordingly, the volume fraction of the crystalline polymer phase, φ_c, was calculated from the known values of ω_c, ρ_c, and ρ:

$$\varphi_c = \omega_c / (\rho_c / \rho) \qquad (27)$$

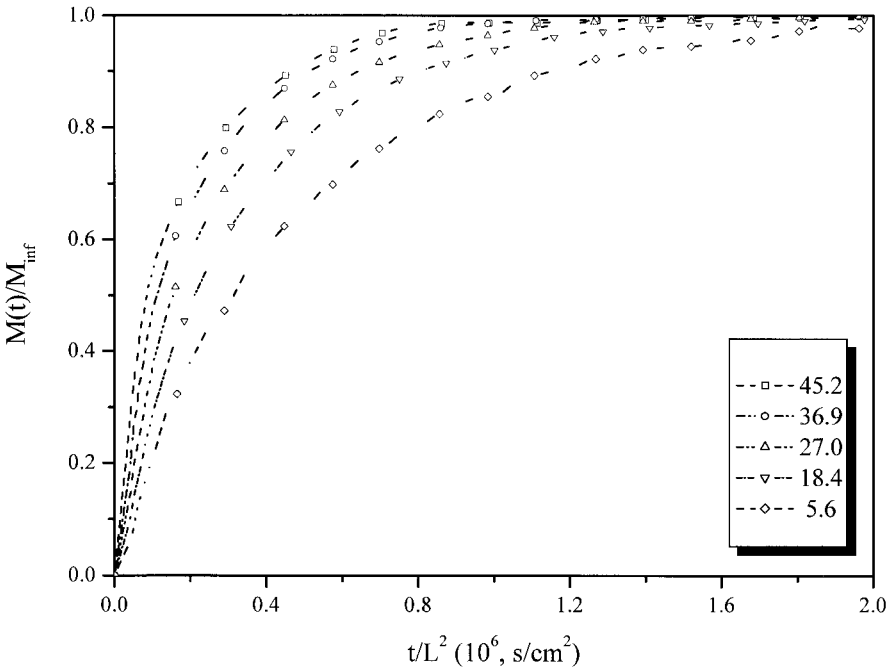

Figure 3 Measured reduced sorption isotherms for the ethylene-polyethylene system (ω_c = 0.738, at 50°C).

For the measurement of an ethylene sorption isotherm, the PE film was first placed in the sample basket and the measuring cell was degassed for approximately 24 h. Subsequently, the measuring cell and the ethylene feeding tank were heated to the desired temperature while the pressure in the ethylene tank was set to a predetermined value. When the specified conditions (e.g., temperature and pressure) were reached, the measuring cell was connected to the ethylene feeding tank and the recording of the sorbed ethylene mass by the PE film was automatically initiated. During the experiments, the temperature and pressure in the measuring cell were continuously monitored to ensure the satisfaction of the specified isothermal and isobaric conditions. After equilibrium had been reached, the gas inlet valve was closed and the measuring cell was degassed until the complete desorption of ethylene from the polymer sample. In Figure 3, typical reduced ethylene sorption curves are depicted at different pressures and a constant temper-

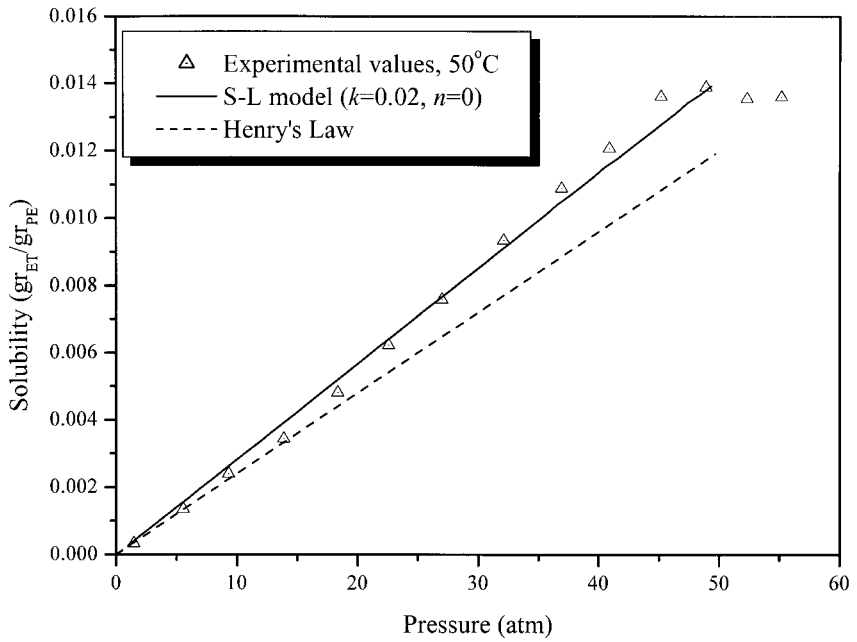

Figure 4 Experimental and predicted values of ethylene solubility as a function of ethylene pressure at T = 50°C.

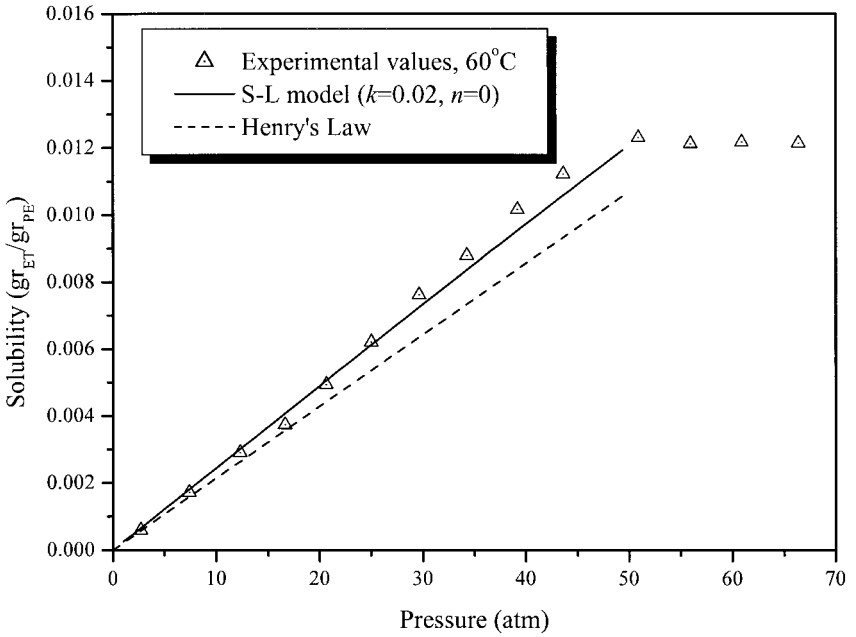

Figure 5 Experimental and predicted values of ethylene solubility as a function of ethylene pressure at T = 60°C.

ature (T = 50°C). It can be seen that the equilibrium sorbed mass of ethylene increases as the ethylene gas pressure increases. However, at ethylene pressures of about 50 atm, the equilibrium mass of sorbed ethylene mass reaches a maximum value due to the presence of the crystalline polymer phase, which hinders the swelling of the amorphous polymer phase.

RESULTS AND DISCUSSION

Ethylene solubility measurements

A number of sorption experiments was carried out to determine the solubility of ethylene in semicrystalline PE films (e.g., ω_c = 0.738). The sorption measurements were carried out at three different temperatures (e.g., 50, 60, and 80°C) and ethylene gas pressures up to 66 atm. From the measured equilibrium values of sorbed ethylene (e.g., Fig. 3), the solubility coefficient of ethylene in PE, S, was experimentally determined.

In Figures 4, 5, and 6, the measured values of ethylene solubility (shown by the discrete points) are plotted with respect to the variation of the ethylene pressure at constant temperature (e.g., 50, 60, and 80°C). For all temperatures studied, the experimentally measured ethylene solubilities reached, at a pressure of about 50 atm, a maximum plateau value that

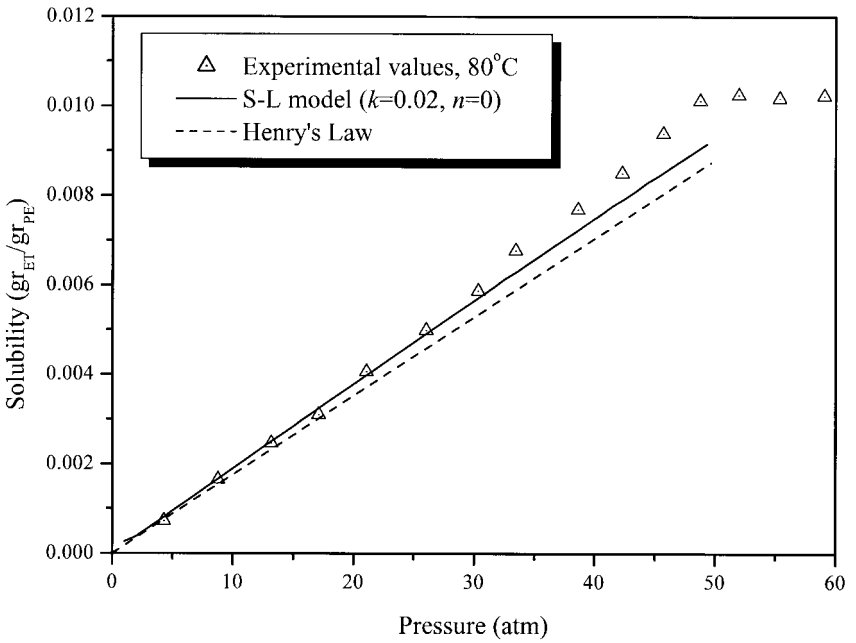

Figure 6 Experimental and predicted values of ethylene solubility as a function of ethylene pressure at T = 80°C.

TABLE I
Pure Component and Segment Parameters Used in the Sanchez–Lacombe Model

Parameter	Polyethylene	Ethylene
T^* (K)	649	294
P^* (bar)	4250	3396
ρ^* (kg/m^3)	904	682

decreased with increasing temperature. From the results of Figures 4–6, it can be seen that the maximum value of ethylene solubility decreases from 1.36×10^{-2} to 1.02×10^{-2} g_{Et}/g_{pol} as the temperature increases from 50 to 80°C. The fact that the ethylene solubility reaches a plateau value at higher pressures can be attributed to the finite degree of swelling of the amorphous PE phase due to the presence of crystalline PE. The crystallites are considered to act as physical crosslinks that limit the swelling of the amorphous polymer phase and, thus, the amount of sorbed ethylene. Li and Long[4] predicted a similar behavior for the solubility of ethylene in PE, but at higher pressures due to the lower crystallinity of the PE sample.

The experimentally determined ethylene solubilities were compared with the theoretical values predicted by both the Henry's law [see eq. (2)] and the S–L lattice-fluid model [eqs. (5)–(15)]. In Table I, the values of the characteristic parameters T^* and P^* and ρ^* for ethylene and PE, used in the S–L model calculations, are reported. In Table II, the estimated values of the Henry's law constant, k^* [see eq. (3)], are reported for three different temperatures. From the results of Figures 4–6, it can be deduced that, at pressures higher than 20 atm, the Henry's law predictions significantly deviate from the experimentally measured ethylene solubilities. On the other hand, the S–L predictions are in good agreement with the experimental ethylene solubilities over the whole range of pressure variation. It should be pointed out that in all S–L model calculations, the values of the binary parameters n and k in eqs. (10)–(11) were kept constant and independent of temperature (e.g., $n = 0.0$ and $k = 0.02$). However, both models (e.g., Henry's law and S–L model) failed to predict the experimentally observed maximum plateau value of the ethylene solubility since both models do not account for the effect of the crystalline amount on the degree of swelling of the amorphous PE phase.

In accordance with the regular solution theory proposed by Hildebrand and coworkers (1949),[32] the solubility of a solute in a solvent is likely to increase as the difference between the respective solubility parameters decreases. In Figure 7, the absolute value of the difference between the ethylene, δ_{Et}, and the polyethylene, δ_{PE}, solubility parameters is plotted with respect to ethylene pressure at three different temperatures. The ethylene solubility parameter, δ_{Et}, was calculated from the solution of the S–L equation of state.[28,32] Notice that the value of δ_{Et} increases as the density of ethylene increases (e.g., the pressure increases or/and the temperature decreases). Assuming that the solubility parameter of the PE remains constant [$\delta_{PE} = 7.9$ (cal/cm^3)$^{1/2}$], it can be easily deduced that the amount of sorbed ethylene increases as the value of $|\delta_{Et} - \delta_{PE}|$ decreases, which is in agreement with the results of Figures 4–6.

Ethylene diffusivity measurements

The mean values of ethylene diffusivity in semicrystalline PE films were estimated from the reduced sorption curves (see Fig. 3), using the half-time method[34]

$$\bar{D} = 0.049/(t_{1/2}/L^2) \tag{28}$$

where L is the thickness of the PE film and $t_{1/2}$ corresponds to the time at which the sorbed ethylene mass is equal to the half of its final equilibrium value.

In Figures 8–9, experimentally determined mean values of ethylene diffusivity (shown by the discrete points) are plotted with respect to the ethylene volume fraction in the amorphous PE phase at different temperatures. Continuous lines represent the values of the ethylene diffusivity predicted by the present diffusion model [eqs. (17)–(25)]. It is apparent that the ethylene diffusion coefficient decreases with temperature and increases with the sorbed ethylene concentration (e.g., the ethylene pressure). The numerical values of all physical parameters used in the diffusion model calculations are shown in Table III. As can be seen, model predictions are in very good agreement with the experimental values of ethylene diffusivity. It should be pointed out that the only parameter that changes with temperature is the mean diffusion jump length ($\bar{L}$). In fact, when the temperature increases from 60 to 80°C, the respective value of $\bar{L}$ varies from 5.5 to 4.7 nm. The dependence of $\bar{L}$ on temperature actually reflects the effect of temperature of ΔE [see eq. (19)]. As shown in Figure 10, the minimum energy, ΔE, required for the effective separation of polymer chains decreases with temperature and, therefore, the probability of a penetrant molecule jump to an adjoining tube increases.

The predictive capabilities of the present diffusion model were further tested by a direct comparison of model predictions with experimental measurements

TABLE II
Henry's Law Constants Calculated by eq. (3)

Temperature (K)	k^* (mol/cm$^3_{am.pol.}$/atm)	k^* (gr/gr $\cdot$ $_{pol}$/atm)
323	2.78E − 5	2.4E − 4
333	2.49E − 5	2.14E − 4
353	2.04E − 5	1.76E − 4

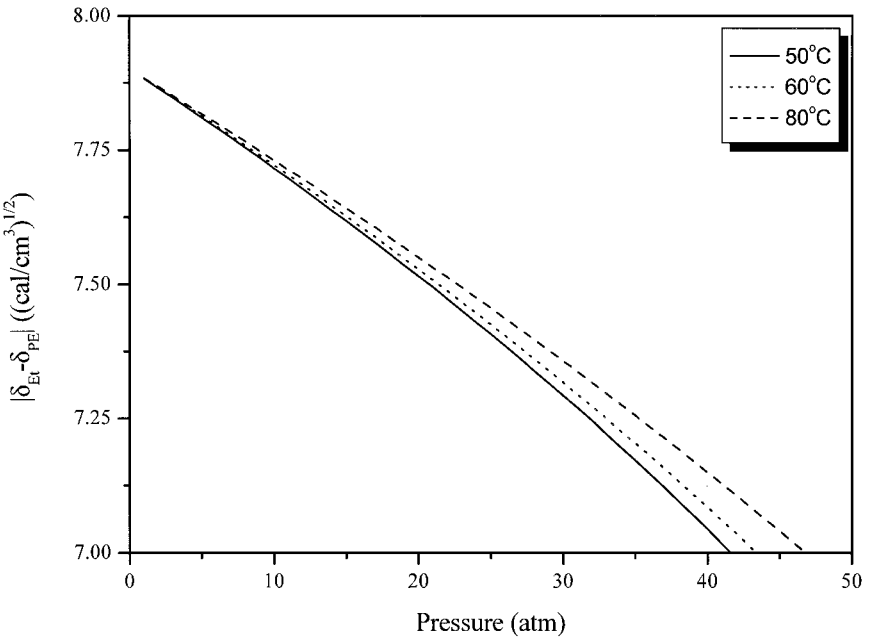

Figure 7 Variation of the absolute value of the difference between ethylene and PE solubility parameters with respect to ethylene pressure.

of ethylene diffusion coefficient in semicrystalline PE (ω_c = 0.48) reported by Beret and Hager[5] (see Fig. 11). In the diffusion model calculations, the value of L was taken to be equal to 12 nm due to the lower degree of polymer crystallinity. Thus, one may conclude that the effect of polymer crystallinity can accurately be described through the variation of the mean diffusion jump length.

CONCLUSIONS

Sorption measurements of ethylene in semicrystalline PE films have shown that ethylene solubility in semicrystalline PE films increases with ethylene concentration and decreases with temperature. The Sanchez–Lacombe lattice fluid model has been employed to describe the dependence of ethylene solubility on tem-

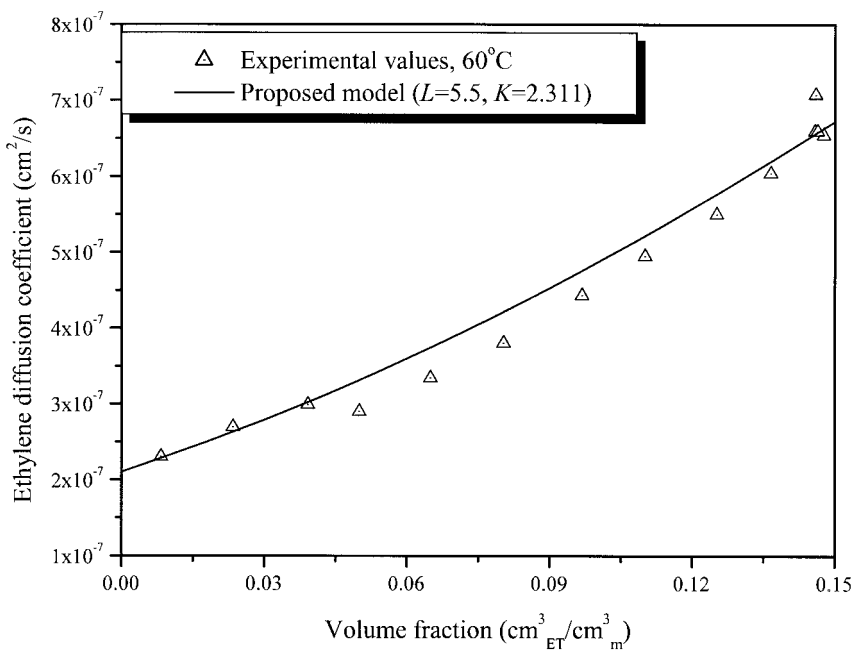

Figure 8 Experimental and predicted values of ethylene diffusion coefficient in semicrystalline polyethylene as a function of ethylene concentration in amorphous PE at T = 50°C.

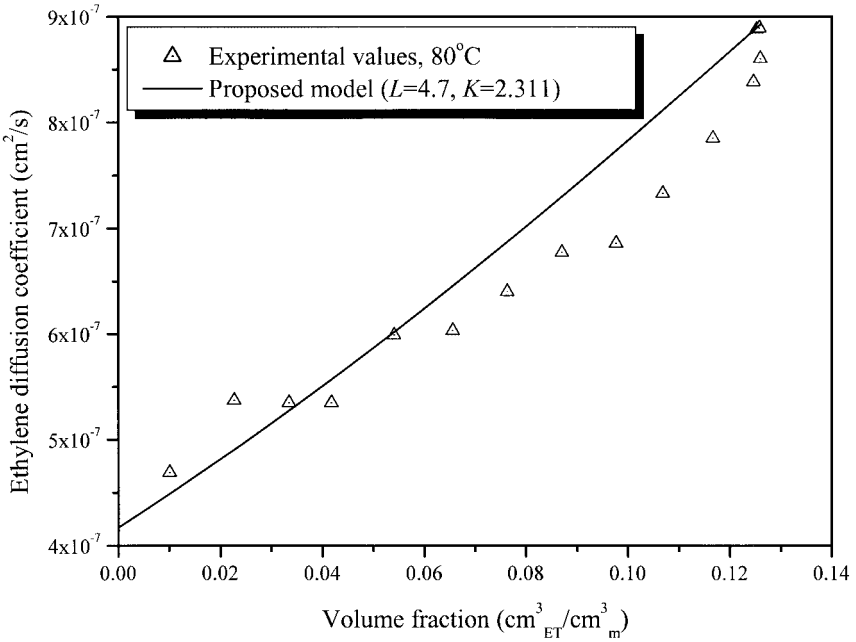

Figure 9 Experimental and predicted values of ethylene diffusion coefficient in semicrystalline polyethylene as a function of ethylene concentration in amorphous PE at $T = 60$°C.

perature and pressure (e.g., ethylene concentration). The experimental solubility measurements were in good agreement with the model predictions at low and moderate pressures. On the other hand, at high pressures, the ethylene solubility reached a plateau value due to the finite degree of swelling of the amorphous PE phase. The ethylene diffusivity in semicrystalline PE was found to increase with temperature and ethylene concentration. A hybrid diffusion model, combining the main features of the Pace–Datyner diffusion model with those of the free-volume model, was developed to assess the effects of temperature, ethylene concentration, and degree of PE crystallinity on ethylene diffusivity. Experimental measurements and model predictions were found to be in good agreement. As a result, the proposed model can successfully be employed for predicting the ethylene diffusivity and, thus, the particle growth in heterogeneous Ziegler–Natta gas-phase olefin polymerizations.

NOMENCLATURE

A_d	Characteristic free-volume parameter (mol m^2/s/J)
B_d	Characteristic free-volume parameter (dimensionless)
b	Positive constant (gr-polymer/gr-penetrant)
C	Concentration of penetrant (gr-penetrant/gr-polymer)
d	Approximate penetrant diameter (nm)
D_{eff}	Effective diffusion coefficient (cm^2/s)
D_d	Thermodynamic diffusion coefficient at zero concentration (cm^2/s)
$\bar{D}$	Experimental mean diffusion coefficient (cm^2/s)

TABLE III
Numerical Values of the Parameters Appearing in the Diffusion Model [eqs. (17)–(25)]

	Polyethylene	Ethylene
ε^* (J mol^{-1})	308	—
ρ^* (nm)	0.463	—
$(\rho^*/\rho)_{\text{ref}}$	1.00	—
$T_{\text{ref.}}$ (K)	298	—
$\beta \times 10^{-3}$ (J nm mol^{-1})	12.0	—
m^* (Da)	14.0	—
λ (nm)	0.1267	—
Noncrystalline density (gr/cm^3)	0.855	—
Collision diameter, σ (nm)	—	0.4163
Lennard–Jones energy parameter, ε/k (K)	—	224.7

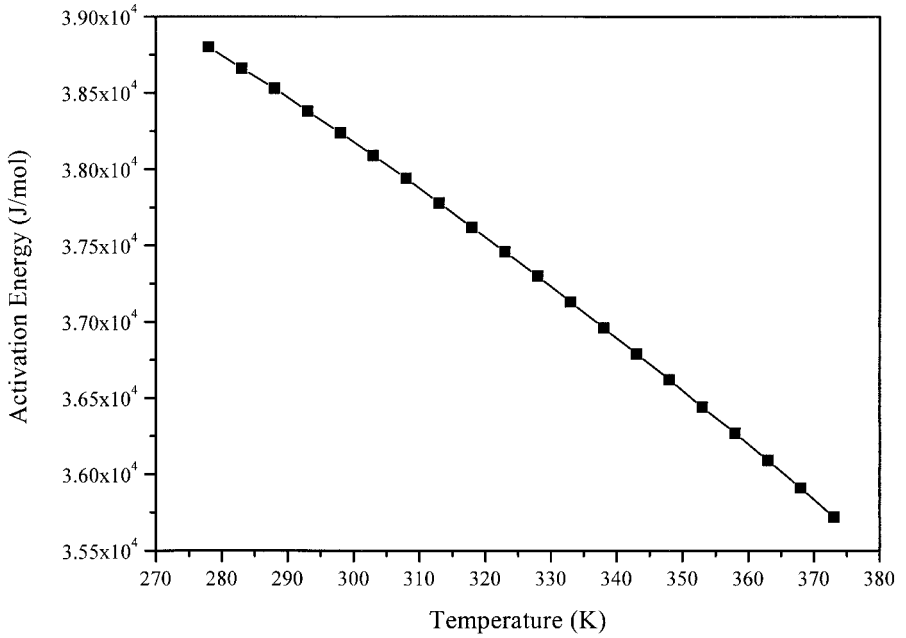

Figure 10 Variation of the minimum activation energy, ΔE [see eq. (19)], with respect to temperature.

k_{ij}	Interaction parameter, Sanchez–Lacombe model (dimensionless)	l^*	Lennard–Jones distance parameter for the polymer (nm)
k^*	Henry's law constant (mol/cm^3-amorphous polymer/atm)	l_0	Mean separation between polymer chains, evaluated from the polymer density (nm)
L	Thickness of the polymer film (cm)	m_i	Mass fraction of component i in the mixture, Sanchez–Lacombe model
$\bar{L}$	Mean diffusion jump length (nm)		
I	Local equilibrium chain separation distance (nm)	m^*	Mass of backbone element (dalton)
		M	Molecular weight (gr/mol)

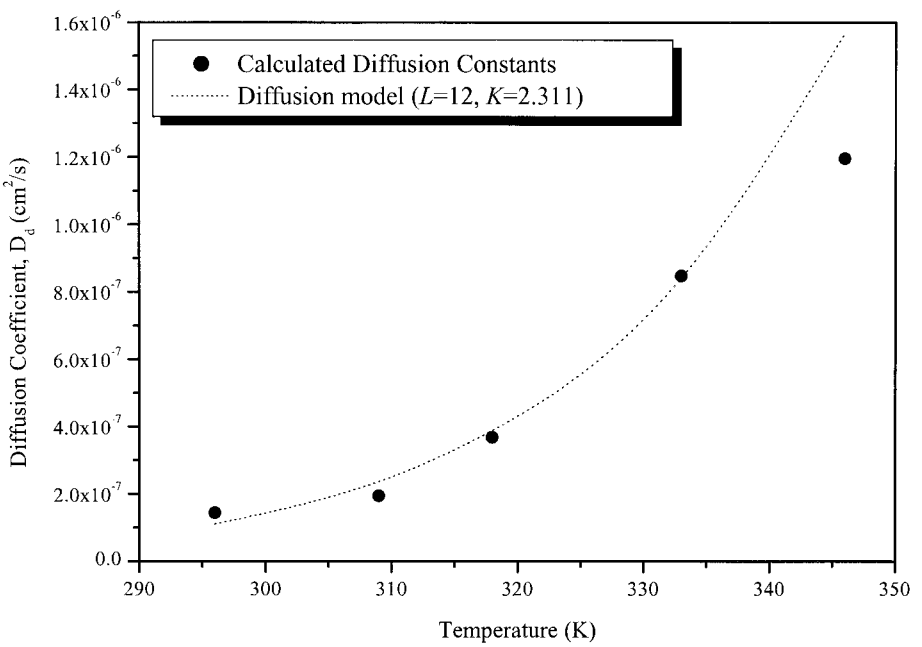

Figure 11 Experimental and predicted values of ethylene diffusion coefficient in semicrystalline polyethylene as a function of temperature.

$[M]^*$ Penetrant concentration in amorphous polymer (mol/cm^3-amorphous polymer)
N Number of molecules, Sanchez–Lacombe model
N_c Number of components in mixture
n_{ij} Interaction parameter, Sanchez–Lacombe model (dimensionless)
P Penetrant pressure (atm)
$\tilde{P}$ Reduced pressure, Sanchez–Lacombe model (dimensionless)
P^* Characteristic parameter, Sanchez–Lacombe model (atm)
r Pure component parameter, Sanchez–Lacombe model (dimensionless)
r_{mix} Mixture parameter, Sanchez–Lacombe model (dimensionless)
R Universal gas constant (J/K/mol)
S Solubility coefficient (mol/cm^3-polymer/atm) or (gr/gr-pol./atm)
S^* Equilibrium solubility coefficient (mol/cm^3-amorphous polymer/atm) or (gr/gr-am.pol./atm)
t Time (s)
T Absolute temperature (K)
$\tilde{T}$ Reduced temperature, Sanchez–Lacombe model (dimensionless)
T^* Characteristic parameter, Sanchez–Lacombe model (K)
T_c Critical temperature of the gas or the vapor (K)
T_g Glass transition temperature (K)
V_f Fractional free volume of the system (dimensionless)
V_{fg} Fractional free volume of the polymer at glass transition temperature (dimensionless)
V_f^* Fractional free volume of the pure polymer as a function of temperature (dimensionless)
x_m Minimum distance between a penetrant molecule and the nearest chain center on a neighboring polymer chain (nm)

Greek letters

α Thermal expansion coefficient (deg^{-1})
β Chain bending modulus (J nm/mol)
γ Concentration coefficient (dimensionless)
δ_{Et} Solubility parameter of ethylene [(cal/cm^3)$^{1/2}$]
δ_{PE} Solubility parameter of PE [(cal/cm^3)$^{1/2}$]
ΔE Activation energy for diffusion (J/mol)
E^* Lennard–Jones energy parameter of backbone element on polymer chain (J/mol)
$\varepsilon_{\mathrm{P}}^*$ Lennard–Jones energy parameter of penetrant (J/mol)
ε^* Mer–mer interaction energy, Sanchez–Lacombe model (J/mol)
$\varepsilon_{\mathrm{mix}}^*$ Interaction energy of the mixture, Sanchez–Lacombe model (J/mol)
λ Backbone element separation along chain (nm)
μ_i^{Polymer} Chemical potential of a component in the polymer (liquid) phase
μ_i^{gas} Chemical potential of a component in the gas phase
$\tilde{\nu}$ Reduced volume, Sanchez–Lacombe model (dimensionless)
$\nu^{*\cdot}$ Close-packed molar volume of a mer, Sanchez–Lacombe model (cm^3/mol)
ν_{mix}^* Close-packed molar volume of a mer of the mixture, Sanchez–Lacombe model (cm^3/mol)
ρ Absolute density (kg/m^3)
$\tilde{\rho}$ Reduced density, Sanchez–Lacombe model (dimensionless)
ρ^* Characteristic close-packed mass density, Sanchez–Lacombe model (kg/m^3)
φ_α Volume fraction of amorphous content of the semicrystalline polymer
φ_c Volume fraction of crystalline content of the semicrystalline polymer
φ_1 Equilibrium volume fraction of penetrant in amorphous polymer
ω_α Weight fraction of amorphous content of the semicrystalline polymer
ω_c Weight fraction of crystalline content of the semicrystalline polymer

References

1. Michaels, A. S.; Parker, R. B., Jr. J Polym Sci 1959, 41, 53.
2. Michaels, A. S.; Bixler, H. J. J Polym Sci 1961, 50, 393.
3. Rogers, C. E.; Stanett, V.; Szwarc, M. J Polym Sci 1960, 45, 61.
4. Li, N. N.; Long, R. B. AIChE J 1969, 15, 73.
5. Beret, S.; Hager, S. L. J Appl Polym Sci 1979, 24, 1787.
6. Kulkarni, S. S.; Stern, S. A. J Polym Sci, Polym Phys Edit 1983, 21, 441.
7. Castro, E. F.; Gonzo, E. E.; Gottifredi, J. C. J Membr Sci 1987, 31, 235.
8. Hutchinson, R. A. Ph.D. Thesis, The University of Wiskonsin–Madison, 1990.
9. Yoon, Y. S.; Chung, C. Y.; Lee, I. H. Eur Polym J 1994 30 (11), 1209.
10. Nath, A. K.; de Pablo, J. J. J Phys Chem 1999, 103, 3539.
11. Sato, Y.; Fujiwara, K.; Takikawa, T.; Sumarno; Takishima, S.; Masuoka, H. Fluid Phase Equilib 1999, 162, 261.
12. Barrer, R. M. J Phys Chem 1957, 61, 178.
13. Fujita, H. Diffusion in Polymer-Diluent Systems, Fortschr. Hochpolym.—Forsch. Bd. 1961, 3, S.1–47.
14. Cohen, M. H.; Turnbull, D. J Chem Phys 1959, 31 (5), 1164.
15. Michaels, A. S.; Bixler, H. J. J Polym Sci 1961, 50, 413.
16. Robeson, L. M.; Smith, T. G. J Appl Polym Sci 1968, 12, 2083.
17. Pace, R. J.; Datyner, R. J Polym Sci, Polym Phys Ed 1979a, 17, 437.
18. Pace, R. J.; Datyner, R. J Polym Sci, Polym Phys Ed 1979b, 17, 453.
19. Pace, R. J.; Datyner, R. J Polym Sci, Polym Phys Ed 1979c, 17, 465.
20. Vrentas, J. S.; Duda, J. L. Macromolecules 1976, 9, 785.
21. Kreituss, A.; Frisch, H. L. J Polym Sci, Polym Phys Ed 1981, 19, 889.
22. Doong, S. J.; Winston, W. S.; Ho, Ind Eng Chem Res 1992, 31, 1050.

23. Schlotter, N. E.; Furlan, P. Y. Polymer 1992, 33, 3323.
24. Hutchinson, R. A.; Ray, W. H. J Appl Polym Sci 1990, 41, 51.
25. Stern, S. A.; Mullhaupt, J. T.; Gareis, P. J. AIChE J 1969, 15, 1, 64.
26. Chen, C. M. Ph.D. Thesis, University of Wisconsin–Madison, 1991.
27. Orbey, H.; Bokis, C.; Chen, C. C. Ind Eng Chem Res 1998, 37, 4481.
28. Briscoe, B. J.; Lorge, O.; Wajs, A.; Dang, P. J Polym Sci, Part B: Polym Phys 1998, 36, 2435.
29. Sanchez, I. C.; Lacombe, R. H. J Phys Chem 1976, 80, 2352.
30. Lacombe, R. H.; Sanchez, I. C. J Phys Chem 1976, 80, 2568.
31. Sanchez, I. C.; Lacombe, R. H. Macromolecules 1978, 11, 1145.
32. McHugh, M.; Krukonis, V. Supercritical Fluid Extraction, 2nd ed.; Butterworth-Heinemann: Stoneham, MA, 1994.
33. Pace, R. J.; Datyner, R. J Polym Sci, Polym Phys Ed 1979d, 17, 1675.
34. Crank, J. The Mathematics of Diffusion, 2nd ed.; Oxford Univ. Press: Oxford, 1975.